





The *Vibrio cholerae* Quorum-Sensing Protein VqmA Integrates Cell Density, Environmental, and Host-Derived Cues into the Control of Virulence

 Ameya A. Mashruwala,^{a,b}  Bonnie L. Bassler^{a,b}

^aDepartment of Molecular Biology, Princeton University, Princeton, New Jersey, USA

^bThe Howard Hughes Medical Institute, Chevy Chase, Maryland, USA

ABSTRACT Quorum sensing is a chemical communication process in which bacteria use the production, release, and detection of signal molecules called autoinducers to orchestrate collective behaviors. The human pathogen *Vibrio cholerae* requires quorum sensing to infect the small intestine. There, *V. cholerae* encounters the absence of oxygen and the presence of bile salts. We show that these two stimuli differentially affect quorum-sensing function and, in turn, *V. cholerae* pathogenicity. First, during anaerobic growth, *V. cholerae* does not produce the CAI-1 autoinducer, while it continues to produce the DPO autoinducer, suggesting that CAI-1 may encode information specific to the aerobic lifestyle of *V. cholerae*. Second, the quorum-sensing receptor-transcription factor called VqmA, which detects the DPO autoinducer, also detects the lack of oxygen and the presence of bile salts. Detection occurs via oxygen-, bile salt-, and redox-responsive disulfide bonds that alter VqmA DNA binding activity. We propose that VqmA serves as an information processing hub that integrates quorum-sensing information, redox status, the presence or absence of oxygen, and host cues. In response to the information acquired through this mechanism, *V. cholerae* appropriately modulates its virulence output.

IMPORTANCE Quorum sensing (QS) is a process of chemical communication that bacteria use to orchestrate collective behaviors. QS communication relies on chemical signal molecules called autoinducers. QS regulates virulence in *Vibrio cholerae*, the causative agent of the disease cholera. Transit into the human small intestine, the site of cholera infection, exposes *V. cholerae* to the host environment. In this study, we show that the combination of two stimuli encountered in the small intestine, the absence of oxygen and the presence of host-produced bile salts, impinge on *V. cholerae* QS function and, in turn, pathogenicity. We suggest that possessing a QS system that is responsive to multiple environmental, host, and cell density cues enables *V. cholerae* to fine-tune its virulence capacity in the human intestine.

KEYWORDS *Vibrio cholerae*, VqmA, oxygen, pathogenesis, quorum sensing, redox

Quorum sensing (QS) is a process of cell-cell communication that bacteria use to synchronize group behaviors such as bioluminescence, DNA exchange, virulence factor production, and biofilm formation (1–4). QS depends on the production, release, accumulation, and group-wide detection of extracellular signaling molecules called autoinducers (AIs) (3, 5). At low cell density (LCD), when there are few cells present and the concentration of AIs is low, the expression of genes driving individual behaviors occurs (3, 5, 6). As the cells grow to high cell density (HCD), the extracellular concentration of AIs likewise increases. Detection of accumulated AIs drives the population-wide expression of genes required for group behaviors.

Vibrio cholerae is a Gram-negative enteric pathogen that causes infectious gastro-

Citation Mashruwala AA, Bassler BL. 2020. The *Vibrio cholerae* quorum-sensing protein VqmA integrates cell density, environmental, and host-derived cues into the control of virulence. mBio 11:e01572-20. <https://doi.org/10.1128/mBio.01572-20>.

Editor Carmen Buchrieser, Institut Pasteur

Copyright © 2020 Mashruwala and Bassler.

This is an open-access article distributed under the terms of the [Creative Commons Attribution 4.0 International license](https://creativecommons.org/licenses/by/4.0/).

Address correspondence to Bonnie L. Bassler, bbassler@princeton.edu.

This article is a direct contribution from Bonnie L. Bassler, a Fellow of the American Academy of Microbiology, who arranged for and secured reviews by Matthew Neiditch, New Jersey Medical School Rutgers, and Jun Zhu, U Penn.

Received 18 June 2020

Accepted 22 June 2020

Published 28 July 2020

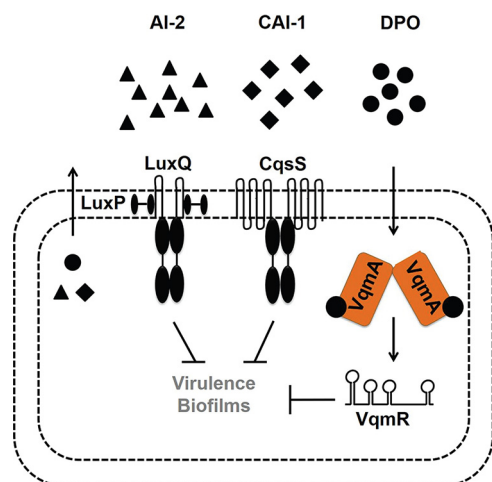


FIG 1 Simplified *V. cholerae* quorum-sensing pathways. See text for details.

enteritis. In *V. cholerae*, QS regulates collective behaviors including virulence factor production and biofilm formation (2, 7–9). Specifically, at LCD, genes encoding virulence factors and those required for biofilm formation are expressed (2). At HCD, genes required for both of these traits are repressed by QS (2). This pattern of gene expression is best understood in the context of the cholera disease. Infection is initiated by the ingestion of a small number of *V. cholerae* cells, and biofilm formation and virulence factor production are required for successful colonization (8, 9). In the host, the growth-dependent accumulation of AIs launches the HCD QS program, which suppresses virulence factor production and biofilm formation, and triggers dispersal of the bacteria back into the environment. Indeed, *V. cholerae* strains “locked” into the LCD QS mode are more proficient in host colonization than strains “locked” in the HCD QS mode (7). Thus, QS is proposed to be crucial for *V. cholerae* transitions between environmental reservoirs and human hosts.

V. cholerae produces and detects three AIs, called AI-2, CAI-1, and DPO (Fig. 1) (2, 10–12). CAI-1 is used for intragenus communication while AI-2 and DPO are employed for interspecies communication (2, 11, 13). Different combinations of the three AIs are thought to allow *V. cholerae* to distinguish the number of vibrio cells present relative to the total bacterial consortium. *V. cholerae* uses the information encoded in blends of AIs to tailor its QS output depending on whether vibrios are in the minority or the majority of a mixed-species population (2, 13).

AI-2 and CAI-1 are detected by the membrane-bound receptors LuxPQ and CqsS, respectively. The receptors funnel information into a shared regulatory pathway (Fig. 1) (2, 10). DPO is detected by the cytoplasmic VqmA receptor-transcription factor that activates expression of *vqmR*, encoding the VqmR regulatory small RNA (sRNA) (11, 14, 15). Both Apo- and DPO-bound-VqmA (Holo-VqmA) can activate *vqmR* expression with Holo-VqmA being more potent than Apo-VqmA (16). VqmR posttranscriptionally regulates target mRNAs (15). Important to this study is that at HCD, all three QS systems repress genes required for virulence and biofilm formation (Fig. 1).

Upon the transition from the marine niche to the human host, *V. cholerae* switches from an aerobic to an anaerobic environment (17, 18). In addition, it encounters bile, which is abundant in the lower intestine, the primary site of *V. cholerae* infection. Bile is a heterogeneous mixture of compounds, including electrolytes and bile acids, and is estimated to be present at ~0.2 to 2% (wt/vol) of intestinal contents (19). Bile salts are known to affect *V. cholerae* virulence gene expression by modulating activities of the oxidoreductase DsbA, the transmembrane-spanning transcription factor TcpP, and the ToxT transcription factor (20–25). Bile salts also promote biofilm formation in *V. cholerae*, and the second messenger molecule called cyclic-di-guanylate is involved in mediating this effect (26, 27).

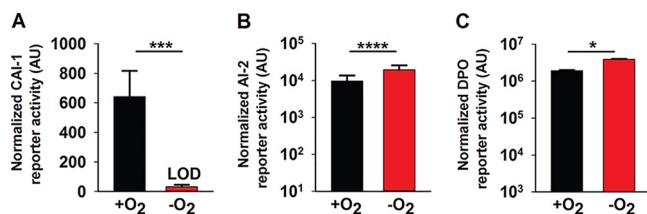


FIG 2 Oxygen deprivation modulates *V. cholerae* AI production. (A) 80%, (B) 25%, or (C) 30% cell-free culture fluids prepared from WT *V. cholerae* grown in the presence or absence of O₂ were provided to *V. cholerae* reporter strains that produce bioluminescence in response to exogenous (A) CAI-1, (B) AI-2, or (C) DPO. Data represent the average values from biological replicates ($n = 3$), and error bars represent SD. Statistical significance was calculated using a two-tailed Student *t* test. Asterisks are as follows: * denotes $P < 0.05$, *** denotes $P < 0.001$, and **** denotes $P < 0.0001$. LOD, limit of detection; AU, arbitrary units.

Here, first we explore whether oxygen levels modulate QS in *V. cholerae*. We find that *V. cholerae* cultured under anaerobic conditions does not produce CAI-1, whereas increased DPO production does occur. In this work, we focus on DPO. We show that the VqmA-DPO complex more strongly activates target gene expression under anaerobic than aerobic conditions. One consequence of the absence/presence of oxygen is an altered reducing/oxidizing (here, redox) cellular environment. We show that oxygen-dependent changes in VqmA activity are governed by cysteine disulfide bonds that are responsive to the redox environment. In the absence of DPO, during aerobic growth, Apo-VqmA forms an intramolecular disulfide bond that limits VqmA activity. In contrast, DPO-bound VqmA forms an intermolecular disulfide bond that enhances VqmA activity, and indeed, this intermolecular disulfide bond was also shown to be present in a recently reported crystal structure of Holo-VqmA (28). The formation of the intermolecular bond is not affected by oxygen levels. In the small intestine, *V. cholerae* encounters both the absence of oxygen and the presence of bile. Bile salts inhibit formation of the intermolecular disulfide bond in VqmA. Thus, bile and DPO have opposing effects on VqmA-DPO activity. We propose that the VqmA-DPO-VqmR QS pathway allows *V. cholerae* to integrate QS information, host cues, and environmental stimuli into the control of genes required for transitions between the human host and the environment.

RESULTS

***V. cholerae* does not produce the CAI-1 QS AI under anaerobic conditions.** To our knowledge, *V. cholerae* QS has been studied only under aerobic conditions. We know that the marine-human host life cycle demands that *V. cholerae* transition between environments containing widely varying oxygen levels (17, 18). Moreover, QS is crucial in both *V. cholerae* habitats. Thus, we sought to investigate whether oxygen modulates *V. cholerae* QS. First, we assessed the relative levels of the three known QS AIs from *V. cholerae* C6706 Sm^r (here wild type [WT]) following aerobic and anaerobic growth. AI activity in cell-free culture fluids was measured using a set of three bioluminescent *V. cholerae* strains, each of which exclusively reports on one QS AI (either AI-2, CAI-1, or DPO) when it is supplied exogenously.

Unlike *V. cholerae* cultured in the presence of oxygen (here +O₂), *V. cholerae* grown in the absence of oxygen (here -O₂) produced no CAI-1 (Fig. 2A). Twice as much AI-2 and DPO accumulated in *V. cholerae* cultured -O₂ as in +O₂ (Fig. 2B and C). We note that the dynamic ranges for the CAI-1 and DPO assay are ~1,000- and ~4-fold, respectively, while that for the AI-2 assay is ~100,000-fold (2, 11). Thus, we consider the changes in CAI-1 and DPO to be physiologically relevant, whereas that for AI-2 is likely not, so we do not consider AI-2 further in this work. Additionally, *V. cholerae* cultured -O₂ grew to a lower final cell density than when grown +O₂ (see Fig. S1A in the supplemental material). We controlled for the reduced cell growth that occurs under the -O₂ conditions; nonetheless, no CAI-1 could be detected (Fig. S1B). Beyond lacking O₂, our culture medium lacked an alternative terminal electron acceptor. Thus, we also

considered the possibility that *V. cholerae* cultured under $-O_2$ conditions was unable to respire and therefore unable to drive CAI-1 generation. However, supplementation of the *V. cholerae* $-O_2$ cultures with the alternative terminal electron acceptor fumarate, which is readily consumed by *V. cholerae* (29), did not rescue CAI-1 production (Fig. S1B). Collectively, these data suggest that production of CAI-1 and DPO by *V. cholerae* is affected by oxygen levels. In the remainder of this study, we focus on the functioning of the DPO-VqmA QS circuit under different conditions that are predicted to be encountered in the host. We address possible ramifications of our results concerning CAI-1 and AI-2 in Discussion.

VqmA exhibits increased activity in the absence of oxygen. Given that *V. cholerae* accumulated more DPO under $-O_2$ conditions than $+O_2$ conditions, we wondered whether the VqmA-DPO QS system would, in turn, display increased activity under $-O_2$ conditions compared to $+O_2$ conditions. VqmA controls the expression of the *vqmR* gene, encoding the small RNA VqmR (Fig. 1). Therefore, expression of a *vqmR-lacZ* transcriptional fusion can be used to assess VqmA activity (11). Beta-galactosidase was selected as the reporter because its activity is not affected by oxygen. The *vqmR-lacZ* construct was integrated onto the chromosome of Δtdh *V. cholerae*. Tdh (threonine dehydrogenase) is required for DPO production (11). Thus, the Δtdh strain makes no DPO but activates *vqmR-lacZ* expression in response to exogenously supplied DPO. We measured activity following growth under $+O_2$ and $-O_2$ conditions and in the absence and presence of exogenous DPO. In the presence of O_2 , *vqmR-lacZ* activity increased following supplementation with DPO (Fig. S2A). Compared to the $+O_2$ conditions, *vqmR-lacZ* activity was higher under $-O_2$ conditions, in both the absence and presence of DPO (Fig. S2A). Increased DPO-independent *vqmR-lacZ* expression in the absence of O_2 could be a consequence of increased production of VqmA or increased VqmA activity. To distinguish between these possibilities, we first examined whether changes in O_2 levels alter VqmA production by quantifying VqmA-FLAG produced from the chromosome $-/+O_2$ and $-/+DPO$. Similar levels of VqmA-FLAG were produced in all cases, suggesting that a change in VqmA abundance does not underlie increased *vqmR-lacZ* expression under $-O_2$ conditions (Fig. S2B). We next tested O_2 -driven changes in VqmA activity. To do this, we uncoupled expression of *vqmA-FLAG* from its native promoter by cloning *vqmA-FLAG* onto a plasmid under an arabinose-inducible promoter (here, *pvqmA-FLAG*). We introduced the plasmid into a $\Delta vqmA \Delta tdh$ *V. cholerae* strain harboring the *vqmR-lacZ* chromosomal reporter, and we measured both β -galactosidase output and VqmA-FLAG abundance in the same samples. VqmA-FLAG levels did not change under the different conditions (Fig. 3A); however, *vqmR-lacZ* reporter activity normalized to cellular VqmA-FLAG levels increased in the cells exposed to DPO, and overall activity was ~ 4 - to 7-fold higher under $-O_2$ conditions than $+O_2$ conditions in both the presence and absence of DPO (Fig. 3B). We conclude that VqmA displays an increased capacity to activate gene expression under anaerobic conditions relative to aerobic conditions.

VqmA forms intra- and intermolecular disulfide bonds in an oxygen- and DPO-dependent manner. We wondered what molecular mechanism drives the increase in VqmA activity under $-O_2$ conditions (Fig. 3). The cytoplasmic compartment of aerobically respiring *V. cholerae* is relatively oxidizing (30, 31). Thus, decreased oxygen levels would shift the cytoplasm to a reducing environment (32). Proteins can respond to such changes via redox-responsive cysteine residues (30, 33). Inspection of the VqmA amino acid sequence revealed the presence of four cysteine residues, and all are strictly conserved in VqmA homologs in other vibrio species, but not in the VqmA receptor recently discovered in a vibriophage (Fig. S3). These findings led us to consider a model in which, in addition to activation by DPO, VqmA activity is regulated by redox-responsive cysteine residues.

Cysteine residues often undergo disulfide bond formation (33–35). We assessed whether VqmA forms disulfide bonds *in vivo* and, if so, whether their formation is influenced by DPO and/or oxygen levels. We grew $\Delta vqmA \Delta tdh$ *V. cholerae* carrying the

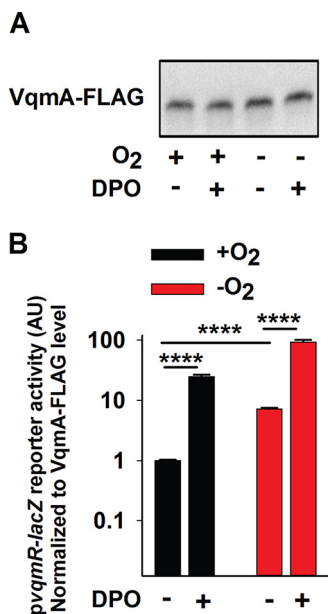


FIG 3 Apo- and Holo-VqmA activities are enhanced in the absence of oxygen. (A) Western blot showing VqmA-FLAG abundance in $\Delta vqmA \Delta tdh$ *V. cholerae* carrying *pvqmA-FLAG* and treated as shown for 1 h. DPO was supplied at 25 μ M. (B) Transcriptional activity for the *pvqmR-lacZ* reporter from the same samples presented in panel A. Data were normalized to the level of VqmA-FLAG in panel A. In panel B, data represent the average values from biological replicates ($n = 3$), and error bars represent SD. Statistical significance was calculated using a two-tailed Student *t* test. Asterisks are as follows: **** denotes $P < 0.0001$.

pvqmA-FLAG construct under +O₂ conditions. We subsequently divided the culture into four aliquots. One portion was untreated (+O₂, -DPO), one portion was supplied with DPO (+O₂, +DPO), one portion was deprived of oxygen (-O₂, -DPO), and one portion was deprived of oxygen and supplemented with DPO (-O₂, +DPO). We extracted protein and analyzed the VqmA-FLAG protein profiles by immunoblotting. These analyses were performed with or without the addition of the reductant β -mercaptoethanol (BME) to distinguish between VqmA-FLAG species that had and had not formed disulfide bonds. Previous studies have shown that the presence of an intramolecular disulfide bond leads to a protein species displaying increased gel mobility compared to the same protein lacking the bond (36, 37). In contrast, intermolecular disulfide bonds produce cross-linked protein oligomers that migrate with lower mobility than the corresponding monomers (35, 38, 39). We first consider the results for VqmA under +O₂ conditions. Under nonreducing conditions (-BME) and in the absence of DPO, VqmA-FLAG displayed mobility consistent with an oxidized monomer (labeled O-Monomer; Fig. 4A and B, lane 1). Treatment with BME caused VqmA-FLAG to migrate more slowly, consistent with it being a reduced monomer (labeled R-Monomer; Fig. 4A and B, lane 2). Administration of DPO drove formation of an additional VqmA-FLAG species, corresponding in size to an oxidized dimer (labeled O-Dimer; Fig. 4A and B, lane 3), but only under oxidizing (i.e., -BME) conditions (Fig. 4B, compare lanes 3 and 4). These results suggest that, under aerobic conditions, a fraction of VqmA harbors an intramolecular disulfide bond and DPO-bound VqmA forms an intermolecular disulfide bond. Under anaerobic conditions, the portion of VqmA containing the intramolecular disulfide bond decreased (Fig. 4B, compare lane 1 to lane 5 and lane 5 to lane 6) while the DPO-dependent intermolecular disulfide-bonded species was unaffected by the absence of oxygen (Fig. 4A, compare lane 3 to lane 7 and lane 7 to lane 8).

To garner additional evidence for the presence of an intramolecular disulfide bond(s) in the species designated VqmA O-monomer in Fig. 4B, we treated samples prepared from cells grown under +O₂ and -DPO conditions with methoxypolyethyl-

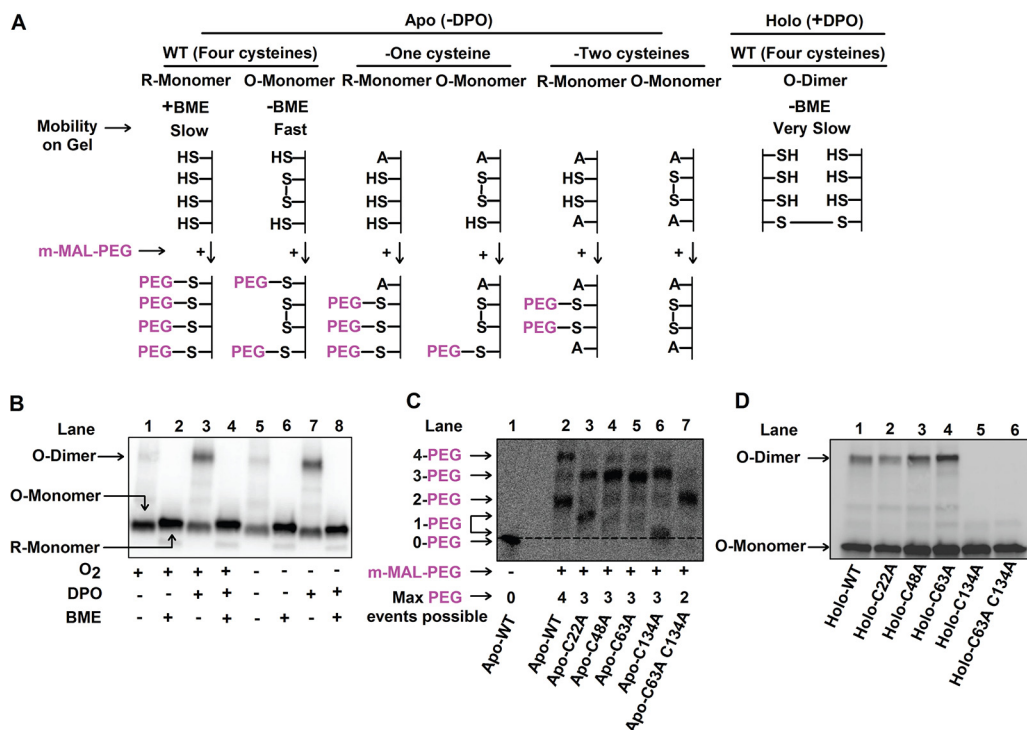


FIG 4 VqmA forms intra- and intermolecular disulfide bonds in an oxygen- and DPO-dependent manner. (A) Schematic depicting the oxidized and reduced forms of VqmA (top) and the strategy employed to interrogate intramolecular disulfide bond formation by trapping reduced thiols with methoxypolyethylene glycol maleimide (m-MAL-PEG; 5 kDa, bottom) (40). (B) Western blot showing VqmA-FLAG protein produced by the $\Delta vqmA \Delta tdh$ *V. cholerae* strain carrying *pvqmA-FLAG* following the specified treatments. (C) Western blot showing VqmA-FLAG protein produced by the $\Delta vqmA \Delta tdh$ *V. cholerae* strain carrying the designated *pvqmA-FLAG* alleles following treatment with m-MAL-PEG (40) in the absence of DPO. Note that in lanes 3 and 6, the proteins containing 1-PEG modification migrate somewhat differently. We infer the bands to be 1-PEG events by comparison with the 0-PEG event in lane 1 and the 2-PEG event in lane 7. A likely explanation is that the protein containing 1-PEG in lane 6 adopts a more compact conformation than the modified protein in lane 3 and so it migrates faster through the gel (36, 37). The dotted line distinguishes the 0-PEG VqmA from the lowest 1-PEG decorated species. (D) Western blot showing VqmA-FLAG for the strains in panel C following supplementation with 25 μ M DPO under nonreducing conditions.

ene glycol maleimide (m-MAL-PEG) (40). m-MAL-PEG alkylates reduced cysteine residues and, in so doing, confers an \sim 5-kDa molecular weight change for each alkylation event (schematic in Fig. 4A). VqmA contains four cysteine residues; thus, the fully reduced protein would undergo 4 m-MAL-PEG events, while if one intramolecular disulfide bond exists, only two cysteine residues could react. Following treatment, Apo-VqmA-FLAG migrated primarily as two bands, corresponding to four (\sim 40% of protein) and two (\sim 60% of protein) alkylation events (Fig. 4C, compare lane 1 to lane 2), confirming that while a portion of VqmA-FLAG is fully reduced *in vivo*, the majority of the protein exists as an oxidized species containing one intramolecular disulfide bond.

To determine the residues involved in VqmA disulfide linkages, we conducted two experiments. First, we employed an *in vitro* thiol-trapping strategy based on sequential reactions that modify accessible cysteine residues with two thiol-specific reagents (Fig. S4A) (41). In the initial thiol-blocking step, purified 6 \times His-VqmA treated with diamide, a thiol-specific oxidant (42), was denatured and incubated with chloroacetamide (CAA). CAA alkylates accessible cysteine residues (i.e., those not involved in disulfide bonds), blocking them from further modification. The CAA-treated sample was next treated with Tris(2-carboxyethyl)phosphine hydrochloride (TCEP), a reductant, enabling non-CAA-labeled cysteines to be reduced. These newly freed residues were labeled in the final alkylation step with *N*-ethylmaleimide (NEM). The sample was then analyzed by mass spectrometry. The logic is that if a particular cysteine residue was

inaccessible to CAA due to disulfide bonding, it would be preferentially labeled with NEM in the subsequent NEM modification step. Thus, the NEM/CAA ratio would be >1 . In contrast, if a cysteine residue was not involved in disulfide modification, it would be preferentially labeled with CAA and have a NEM/CAA ratio of <1 . The VqmA C48 and C63 residues had NEM/CAA ratios of ~ 100 and ~ 10 , respectively, suggesting both of these residues are involved in disulfide linkages (Fig. S4B). We were unable to obtain good coverage of the C134 and C22 residues using this technique, so we could not similarly assess them.

Our second experiment to probe disulfide bonds in VqmA relied on mutagenesis. We individually substituted an alanine residue for each cysteine residue in the *pvqmA-FLAG* construct, introduced the plasmids into the $\Delta vqmA \Delta tdh$ *V. cholerae* strain, and repeated the analyses described in Fig. 4C. We first consider the case of intramolecular disulfide bond formation under $+O_2 -DPO$ conditions. In the mutant proteins, following replacement of a cysteine residue with alanine, a maximum of three residues can react with m-MAL-PEG in the fully reduced protein (Fig. 4A, top). However, if an intramolecular disulfide bond is present, then only one cysteine residue can be decorated with m-MAL-PEG. Figure 4C shows that the Apo-VqmA C22A and Apo-VqmA C134A proteins each migrated as two bands, a result consistent with portions of each protein harboring one and three m-MAL-PEG moieties (Fig. 4C; compare lane 3 to lanes 2 and 1 and compare lane 6 to lanes 2 and 1). This result suggests that the fraction of Apo-VqmA C22A and the fraction of Apo-VqmA C134A that exhibit one m-MAL-PEG decoration harbor intramolecular disulfide bonds. Apo-VqmA C48A and Apo-VqmA C63A migrated largely as single bands at the region corresponding to three m-MAL-PEG decorations (Fig. 4C; compare lanes 4 and 5 to lane 2), suggesting that these proteins exist as reduced species and are thus incapable of forming intramolecular disulfide bonds. Therefore, we conclude that in WT VqmA, an intramolecular disulfide bond is formed between cysteine residues 48 and 63.

Next, we consider intermolecular disulfide bond formation under $+O_2 +DPO$ conditions, and under nonreducing conditions (i.e., $-BME$). Figure 4D shows that the Holo-VqmA C22A, Holo-VqmA C48A, and Holo-VqmA C63A proteins migrated as mixtures of oxidized monomers and oxidized dimers, while the Holo-VqmA C134A protein migrated exclusively as an oxidized monomer (compare lanes 2 to 5 to lane 1). These data suggest that in Holo-VqmA, there is a C134-C134 intermolecular disulfide linkage. We also constructed and assessed the double VqmA C63A C134A mutant under $+O_2 +m-MAL-PEG$ and $+O_2 +DPO$ conditions. Figure 4C shows that under aerobic conditions, all of the Apo-VqmA C63A C134A protein contains two m-MAL-PEG decorations (compare lane 7 to lane 2), confirming that the two remaining cysteine residues were accessible and that the protein is fully reduced. Figure 4D shows that under aerobic conditions Holo-VqmA C63A C134A migrates entirely as a monomer (compare lanes 6 to lane 1). Thus, Holo-VqmA C63A C134A is incapable of forming both intra- and intermolecular disulfide bonds.

Collectively, our data suggest that (i) VqmA forms disulfide bonds *in vivo* and *in vitro*; (ii) an intramolecular disulfide bond is formed between VqmA C48 and C63, and an intermolecular disulfide bond is made between C134 and C134; and (iii) disulfide bond formation is influenced by both oxygen and DPO.

VqmA activity is limited by the intramolecular disulfide bond and enhanced by the intermolecular disulfide bond. To explore the *in vivo* consequences of VqmA disulfide bond formation on VqmA function, we tested whether the Apo- and Holo-mutant VqmA proteins that are incapable of forming particular intra- and/or intermolecular disulfide bonds displayed altered abilities to activate target *vqmR* transcription (see schematic in Fig. S5A). We introduced the *vqmA-FLAG*, *vqmA C48A-FLAG*, and *vqmA C134A-FLAG* alleles onto the chromosome of a *V. cholerae* Δtdh strain carrying *vqmR-lacZ* and measured reporter activity following aerobic growth $+/-DPO$. Our rationale was that WT VqmA forms both the C48-C63 intramolecular bond and the C134-C134 intermolecular bond. In contrast, the VqmA C48A variant is unable to form the C48-C63 intramolecular bond and the VqmA C134A variant is unable to form the C134-C134

intermolecular bond (Fig. 4C and D). Therefore, by comparing the activities of these three proteins, we could assess the effect of individually eliminating each disulfide bond on VqmA activity. We likewise made a strain carrying *vqmA C63A C134A-FLAG* on the chromosome to examine the effect of simultaneous elimination of both disulfide bonds.

First, we consider the case of Apo-VqmA. Apo-VqmA C48A and Apo-VqmA C134A exhibited an ~2-fold and ~4-fold increase and decrease, respectively, in reporter activity, relative to WT Apo-VqmA (Fig. S5B). Apo-VqmA C63A C134A exhibited an ~3-fold increase in reporter activity relative to WT Apo-VqmA and an ~10-fold increase in reporter activity relative to the strain carrying the Apo-VqmA C134A single mutant (Fig. S5B). Thus, we conclude that the C48-C63 intramolecular disulfide bond limits transcriptional activity of Apo-VqmA.

Next, we consider the case for Holo-VqmA. In cultures supplemented with DPO, *vqmR-lacZ* reporter activity increased ~20- to 30-fold, in a DPO-concentration-dependent manner in the strain carrying WT Holo-VqmA relative to the strain with WT Apo-VqmA (Fig. S5C). The strain carrying the VqmA C48A variant displayed a further increase in DPO-dependent reporter activity relative to the WT-VqmA. However, in strains harboring Holo-VqmA C134A and Holo-VqmA C63A C134A, only modest (3- to 4-fold) responses to DPO occurred (Fig. S5C). Thus, the DPO-responsive, C134-C134 intermolecular disulfide bond enhances VqmA transcriptional activation activity.

VqmA activity is differentially modulated by the cellular redox environment.

To test whether VqmA activity is responsive to cellular redox, we supplemented the strains carrying the different VqmA variants with dithiothreitol (DTT), a cell-permeating reductant. We reasoned that if the absence of oxygen generates a reducing environment that prevents the formation of a particular disulfide bond, addition of DTT would mimic this condition by promoting a reducing cellular environment, including in the presence of oxygen. To control for any potential DTT-induced changes in the levels of chromosomally expressed *vqmA*, we introduced plasmids harboring arabinose-inducible *vqmA-FLAG*, *vqmA C134A-FLAG*, or *vqmA C63A C134A-FLAG* into the *V. cholerae* $\Delta vqmA \Delta tdh$ strain carrying *vqmR-lacZ* and measured reporter activity +/- DPO and +/- DTT.

In the absence of DTT, the Apo- and Holo- plasmid-borne VqmA variants displayed reporter activities similar to when the variants were expressed from the chromosome (plasmid-borne variants are in Fig. 5A and B; compare the black bars in each panel; for chromosomal variants, see Fig. S5B and C). Treatment with DTT increased reporter activity for WT Apo-VqmA and Apo-VqmA C134A but did not alter the reporter activity in the strain carrying Apo-VqmA C63A C134A (Fig. 5A, compare black and gray bars for each strain). As a reminder, WT Apo-VqmA and Apo-VqmA C134A form the C48-C63 intramolecular disulfide bond, while the Apo-VqmA C63A C134A protein does not. Thus, these data suggest that a reducing environment interferes with formation of the C48-C63 intramolecular disulfide bond, thereby eliminating its negative effect on Apo-VqmA activity.

Regarding WT Holo-VqmA, reporter activity diminished by ~6-fold when DTT was present in addition to DPO (Fig. 5B; compare the first pair of black and gray bars). In contrast, DTT supplementation did not significantly affect reporter activity in the strain carrying Holo-VqmA C134A (Fig. 5B; compare the second set of black and gray bars), while ~3-fold-lower activity was produced by the strain carrying Holo-VqmA C63A C134A (Fig. 5B; compare the third set of black and gray bars). Since the activity of VqmA C134A was not affected by DTT supplementation, we conclude that the C134-C134 intermolecular bond does not form in a reducing environment, and without that bond, Holo-VqmA transcriptional activity is diminished. Indeed, further emphasizing this conclusion, following DTT administration, reporter activity declined 5-fold in the DPO-treated strain harboring arabinose-inducible *vqmA C48A-FLAG* (Fig. S5D).

VqmA DNA binding capacity is differentially modulated by its redox environment. We suspected that the *in vivo* redox-dependent changes in VqmA disulfide bond formation would have ramifications on VqmA DNA binding capability. To explore this

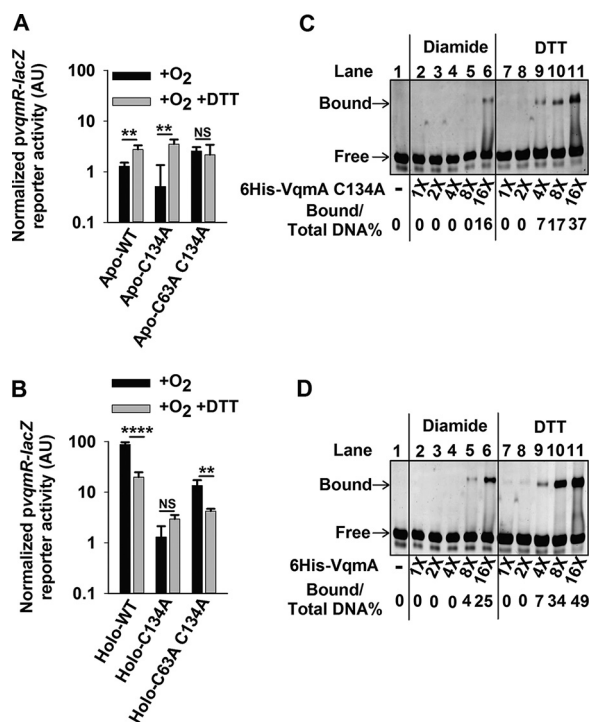


FIG 5 VqmA activity is differentially modulated by the cellular redox environment and intra- and intermolecular disulfide bonds. (A) *pvqmR-lacZ* activity in $\Delta vqmA \Delta tdh$ *V. cholerae* carrying the designated *pvqmA-FLAG* constructs following growth in the presence of O₂ without (black) or with (gray) DTT. (B) Strains cultured as in panel A supplemented with 25 μ M DPO. (C) Electromobility shift analysis (EMSA) of 6xHis-VqmA C134A binding to *pvqmR* promoter DNA. (D) EMSA as in panel C for WT 6xHis-VqmA. In panels C and D, all lanes contained 35 ng of promoter DNA, and where indicated, dilutions of protein were used with 16x = 2 μ g. Bound and free correspond to DNA that is and is not bound to VqmA protein, respectively. As indicated, VqmA had been treated with 10-fold molar excess of diamide or DTT. Data in panels A and B represent average values from biological replicates ($n = 3$), and error bars represent SD. Statistical significance was calculated using a two-tailed Student *t* test. Asterisks are as follows: ** denotes $P < 0.01$, **** denotes $P < 0.0001$, and NS denotes $P > 0.05$.

notion, we examined the ability of purified VqmA proteins to bind *pvqmR* promoter DNA. First, to examine the role of the C48-C63 intramolecular disulfide bond, we assessed DNA binding for 6xHis-VqmA C134A treated with diamide (to enable disulfide bond formation) or DTT (to prevent disulfide bond formation) (see Fig. S6). Relative to the DTT-treated protein, the diamide-treated protein exhibited a 4-fold reduction in DNA binding (Fig. 5C; compare lanes 2 to 6 with lanes 7 to 11). This result suggests that formation of the C48-C63 intramolecular disulfide bond limits DNA binding.

We investigated the role of the VqmA C134-C134 intermolecular disulfide bond on DNA binding by comparing the DNA binding capabilities of 6xHis-VqmA and 6xHis-VqmA C134A. Diamide-treated 6xHis-VqmA was approximately twice as potent at binding DNA as was 6xHis-VqmA C134A (compare left halves of Fig. 5C [VqmA C134A] and Fig. 5D [WT VqmA]), suggesting that the C134-C134 intermolecular disulfide bond promotes DNA binding. The DTT-treated 6xHis-VqmA C134A and 6xHis-VqmA proteins showed no difference in DNA binding capability (compare right halves of Fig. 5C [VqmA C134A] and Fig. 5D [WT VqmA]). Like 6xHis-VqmA C134A, DTT-treated 6xHis-VqmA was more proficient in DNA binding than diamide-treated 6xHis-VqmA, consistent with intramolecular disulfide bond formation limiting DNA binding (Fig. 5D). Collectively, the data in Fig. 4 and 5 suggest a model in which the transcriptional and DNA binding activities of both Apo-VqmA and Holo-VqmA are modulated by disulfide bond formation, the cytoplasmic redox environment, and the level of O₂ in the environment.

Bile salts interfere with VqmA disulfide bond formation and decrease VqmA transcriptional activation activity. Our above findings suggest that the VqmA-DPO

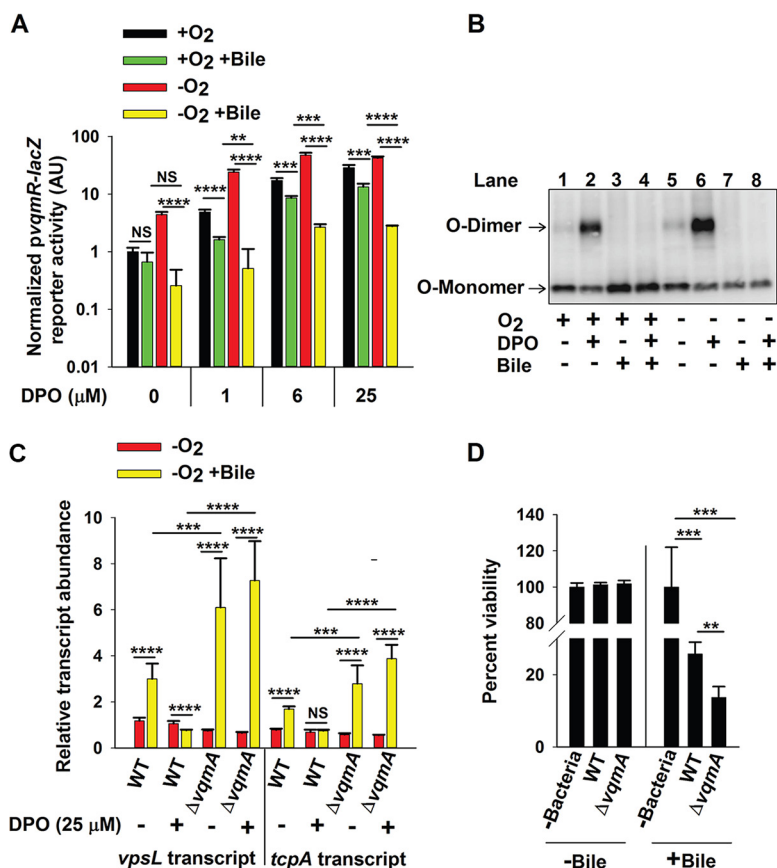


FIG 6 Bile salts disrupt VqmA-DPO-mediated signal transduction and promote *V. cholerae* virulence. (A) *pvqmR-lacZ* activity in $\Delta vqmA \Delta tdh$ *V. cholerae* carrying *pvqmA-FLAG* following 1 h in the presence or absence of O₂, 0.5% (vol/vol) bile salts, and 0 to 25 μ M DPO or combinations of all three treatments as indicated. (B) Western blot showing VqmA-FLAG for the strain in panel A following the indicated treatments. (C) Relative expression levels of *vpsL* and *tcpA* in WT and $\Delta vqmA$ *V. cholerae* following the designated treatments. (D) Viability of human intestinal Caco-2 cells in the absence of bacteria or following challenge by WT or $\Delta vqmA$ *V. cholerae* and in the presence or absence of 0.05% bile salts. Data in panels A and D represent average values from biological replicates ($n = 3$), and error bars represent SD. Data in panel C represent the average value from three biological replicates and two technical replicates for each sample ($n = 6$), and error bars represent SD. Statistical significance was calculated using a two-tailed Student *t* test. Asterisks are as follows: ** denotes $P < 0.01$, *** denotes $P < 0.001$, **** denotes $P < 0.0001$, and NS denotes $P > 0.05$.

signal transduction pathway, which represses virulence factor production and biofilm formation, is most highly active under anaerobic conditions. *V. cholerae* encounters anaerobiosis in the human intestine. The paradox is that in the intestine, *V. cholerae* is virulent and makes biofilms. We thus wondered if a possible host intestinal signal(s) could modulate VqmA-DPO signaling, allowing infection to proceed under anaerobic conditions. Bile salts, present in high concentrations in the human small intestine, can alter the redox environment of bacterial cells and thereby affect disulfide bond formation in cytoplasmic proteins (43). Thus, we were inspired to investigate whether bile salts could abrogate VqmA-DPO transcriptional activation activity. We cultured the $\Delta vqmA \Delta tdh$ *V. cholerae* strain carrying the arabinose-inducible *pvqmA-FLAG* construct and *vqmR-lacZ* on the chromosome in the presence and absence of oxygen, bile, and DPO, and we measured reporter activity. Treatment with bile salts caused ~2-fold and ~10-fold decreases in *vqmR-lacZ* reporter activity under +O₂ and -O₂ growth, respectively (Fig. 6A, first four bars). Supplementation with bile salts also decreased *vqmR-lacZ* reporter activity in cultures supplied with DPO, again with the maximum effect observed under -O₂ growth (Fig. 6A, 5th bar onward). To test whether the presence of bile salts affects VqmA disulfide bonds, we used analyses similar to those in Fig. 4B.

Consistent with the *vqmR-lacZ* reporter activity, bile salt supplementation prevented formation of O-dimers, in both the presence and absence of O₂, suggesting it interferes with the Holo-VqmA C134-C134 intermolecular disulfide bond (Fig. 6B). We do not know whether or not bile affects VqmA intramolecular disulfide bond formation.

Bile salt-mediated disruption of VqmA-DPO-driven signal transduction promotes *V. cholerae* virulence. In *V. cholerae*, VqmA-DPO-directed production of VqmR results in decreased expression of genes involved in biofilm formation and virulence factor expression, including *vpsL* and *tcpA*, respectively (11, 15). *VpsL* is required to synthesize *V. cholerae* exopolysaccharide, an essential component of the biofilm matrix, and *TcpA* is a virulence factor required for *V. cholerae* to colonize the human small intestine (44, 45). Our finding that supplementation with bile salts inhibited VqmA-DPO function and that the effect of bile salt-mediated inhibition occurred primarily in the absence of oxygen led us to predict that the repression of *vpsL* and *tcpA* expression would also be maximally disrupted following bile salt supplementation in the absence of oxygen. We measured transcript levels of *vpsL* and *tcpA* in the WT and $\Delta vqmA$ strains following exposure to 25 μ M DPO or bile salts, deprivation of oxygen, or combinations of the three treatments.

In WT *V. cholerae*, bile salt supplementation modestly increased *vpsL* and *tcpA* transcript levels (\sim 3- and \sim 2-fold, respectively) but, however, only under $-O_2$ -DPO conditions (Fig. 6C and Fig. S7). These data suggest that bile salts induce genes required for biofilm formation and virulence in the absence of oxygen and that Holo-VqmA can override the effect of bile. Transcript levels for both *vpsL* and *tcpA* under $-O_2$ -DPO conditions were further increased in the $\Delta vqmA$ strain treated with bile salts (\sim 6- and \sim 3-fold, respectively). We interpret this result to mean that bile salts also induce an increase in *vpsL* and *tcpA* expression through a pathway that does not involve VqmA. However, because the major effect of bile salts occurs only in the $\Delta vqmA$ strain, we conclude that this additional pathway is epistatic to VqmA in the control of *vpsL* and *tcpA*.

We tested whether the above changes in gene expression translated into alterations in *V. cholerae* pathogenicity by assaying whether bile salts affected cytotoxicity of *V. cholerae* in coculture with human Caco-2 intestinal cells. We generated differentiated monolayers of Caco-2 cells and cocultured them with either WT or $\Delta vqmA$ *V. cholerae* in the presence and absence of bile salts. The presence of bile salts increased *V. cholerae*-mediated cytotoxicity to Caco-2 cells with the $\Delta vqmA$ strain driving twice as much killing as WT *V. cholerae* (Fig. 6D). Collectively, our data suggest that bile salts induce increased *V. cholerae* virulence when bacteria are deprived of oxygen, part of the bile salt effect is exerted via interference with the VqmA-DPO-VqmR QS circuit, and the presence of VqmA limits the ability of bile salts to affect target gene expression.

DISCUSSION

The diversity of environments that *V. cholerae* inhabits, from the ocean to marine organisms to the human stomach to the human intestine, necessitates that the bacterium rapidly perceives changes in its external environment and appropriately tailors its gene expression programs. Our current study reveals that *V. cholerae* alters both which AIs are produced and the functioning of the VqmA-DPO-VqmR QS circuit in response to its environment. To our knowledge, these findings represent the first dissection of QS activity in the absence of oxygen in a facultative aerobic bacterium. We find that (i) the amounts of two AIs (CAI-1 and DPO) produced are dictated by oxygen levels; (ii) a single QS protein (VqmA) is capable of integrating information from three sources (AI, oxygen, and bile salts); and (iii) two disulfide bonds in a QS receptor (VqmA) antagonize one another with respect to their effects on protein activity, thereby aiding in perception and response to changes in cellular redox.

The benefit(s) of producing and detecting multiple QS AIs has long been mysterious with respect to *V. cholerae* biology. Evidence suggests that each AI conveys specific information into the cell: CAI-1 measures the abundance of vibrios (kin) and AI-2 and DPO measure the level of nonvibrios (non-kin) in the vicinity (11, 13, 15). Our finding

that CAI-1 is not produced in the absence of oxygen suggests that CAI-1 may also convey information about the external environment. Strains lacking the ability to synthesize CAI-1 display reduced survival in seawater and following challenge with oxidative stress (46). Thus, we propose that CAI-1 could drive the expression of genes required for the aerobic segment of the *V. cholerae* life cycle, and we are now testing this idea. The fact that CAI-1 is not produced under anoxia suggests that *V. cholerae* cannot take a census of kin in the absence of oxygen. Either kin counting is dispensable under anoxia, or perhaps, another molecule(s)/mechanism performs this function. In contrast, at a minimum based on sequencing data, thousands of bacterial species, including those found in the human microbiota, can synthesize AI-2, the AI used for interspecies communication (47). We found that AI-2 is synthesized in the absence of oxygen. Perhaps measurement of the abundance of non-kin bacteria is of paramount importance in densely populated niches containing complex bacterial consortia. Bio-synthesis of both AI-2 and CAI-1 requires S-adenosylmethionine (SAM), an abundant metabolite that is crucial for methylation reactions (12, 48, 49). Thus, another possibility is that in *V. cholerae*, during periods of SAM limitation, CAI-1 production is curbed as a means of sparing SAM for other uses. Continued AI-2 production could suffice for QS-mediated cell density tracking. Moreover, when SAM is used to produce AI-2 but not CAI-1, SAM is regenerated via downstream reactions (12, 50). Thus, making AI-2 from SAM would not deplete the SAM reservoir.

Oxygen is a terminal electron acceptor and therefore a critical substrate for bacterial growth. The human intestine is devoid of oxygen, and invading bacteria, such as *V. cholerae*, that normally inhabit the relatively oxygenated marine environment need to alter their physiology to survive. With the exception of a few studies (30, 51, 52), the molecular mechanisms by which *V. cholerae* perceives the absence of oxygen and translates this information into changes in gene expression are unexplored. Here, we demonstrate that, in the presence of O₂, Apo-VqmA forms a C48-C63 intramolecular disulfide bond that restricts the ability of the protein to bind DNA. Formation of this bond is inhibited in the absence of oxygen or following supplementation of aerobic cells with a reductant that, analogous to the absence of oxygen, generates a reducing environment. Thus, we propose that by interacting with the cell's redox environment, VqmA provides *V. cholerae* a mechanism to monitor oxygen levels (Fig. 7A). In this context, we note that anaerobiosis causes an ~7-fold increase in Apo-VqmA-dependent *pvqmR-lacZ* reporter activity (Fig. 3B). In contrast, DTT supplementation under aerobic conditions causes only an ~3-fold increase in Apo-VqmA activity while the activity of Apo-VqmA C63A C134A, which lacks both disulfide bonds, is unchanged (Fig. 5A). One interpretation of these data is that Apo-VqmA is responsive to additional oxygen-dependent stimuli that are not mimicked by DTT or by the inability to make disulfide bonds. We are currently testing this possibility.

With respect to DPO-bound VqmA, we found that Holo-VqmA forms a C134-C134 intermolecular disulfide bond. Our data expand on a recent study of VqmA in which the crystal structure revealed the C134-C134 disulfide bond in Holo-VqmA. The authors predicted that the C134-C134 bond could interfere with VqmA DNA binding (28, 53). However, the role of the disulfide bond on VqmA activity was not experimentally investigated in that earlier work (28). Here, we show that the C134-C134 bond is largely absent in Apo-VqmA while, upon binding DPO, ~40 to 50% of Holo-VqmA undergoes intermolecular C134-C134 disulfide bond formation, and moreover, this bond promotes Holo-VqmA activation of transcription (Fig. 4B and Fig. 5). We do not understand why the conclusion one naturally comes to from the crystal structure does not match the experimental data. We do note that the C134 residue is located in a flexible loop region. Thus, one possibility is that, in the static crystal, the loop region is spatially constrained and does not reflect dynamic structures that VqmA adopts in solution. This notion awaits experimental testing.

Our results show that formation of the C134-C134 bond is not modulated by oxygen levels but is inhibited by the reductant DTT. The absence of oxygen imposes a mildly reducing environment on cells, while the presence of DTT imposes reductive stress (32,

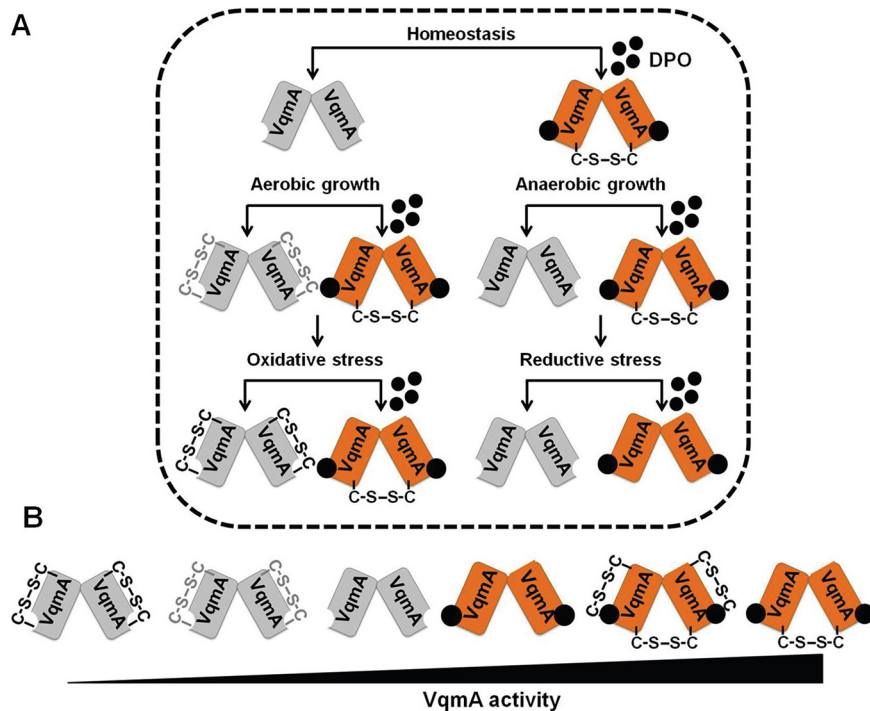


FIG 7 Model depicting VqmA as a hub protein that compiles quorum sensing, environmental, and host information. (A) VqmA can exist in different states *in vivo* depending upon the availability of the DPO ligand and the cellular redox state. Thus, Apo-VqmA forms the C48-C63 intramolecular disulfide bond that suppresses its ability to bind DNA. Apo-VqmA activity is high under reducing growth conditions in which formation of the intramolecular C48-C63 bond is inhibited. Holo-VqmA forms the C134-C134 intermolecular disulfide bond that promotes DNA binding. Reductive stress disrupts the formation of the intermolecular disulfide bond. We propose that growth in the presence of bile salts imposes reductive stress, disrupts the formation of the C134-C134 intermolecular disulfide bond, and restricts VqmA DNA binding, thereby promoting virulence and biofilm formation. The gray and black intramolecular disulfide bonds denote partially oxidized and fully oxidized VqmA, respectively. (B) Relative VqmA activity levels as a consequence of disulfide bond formation. For simplicity, the fourth and fifth species in panel B are not displayed in panel A.

54), suggesting that the C134-C134 intermolecular VqmA disulfide bond may allow *V. cholerae* to monitor reductive stress. Under *in vitro* conditions, the negative effect exerted by the C48-C63 intramolecular disulfide bond on DNA binding was more significant than the positive effect exerted by the C134-C134 intermolecular disulfide bond. This result contrasts with our *in vivo* data (Fig. 5B), in which the intermolecular disulfide bond has the most pronounced effect on WT VqmA activity. One explanation that we are now exploring is that *in vivo*, additional factors modulate the activity of WT VqmA containing the intermolecular disulfide bond. Collectively, we suggest a model in which cycling between multiple redox states, namely, Oxidized-Apo-VqmA, Reduced-Apo-VqmA, Oxidized-Holo-VqmA, and Reduced-Holo-VqmA, enables *V. cholerae* to tune its QS-controlled collective behaviors to a range of redox states (Fig. 7B). There exist examples of individual disulfide bonds restricting or enhancing the activity of transcription factors (55–57). To our knowledge, however, this is the first example in which the same protein simultaneously uses two different disulfide bonds to modulate activity.

Bile is an abundant compound in the human small intestine that is well known to alter virulence in *V. cholerae* and other enteric pathogens such as *Salmonella enterica* serovar Typhimurium and *Shigella flexneri* (58, 59). Bile is a heterogeneous mixture of molecules, and studies have largely focused on defining the roles of individual components in bacterial physiology. Intriguingly, the individual components can drive opposing effects. In *V. cholerae*, bile fatty acids repress while the bile salt taurocholate induces virulence (20–22, 25, 60, 61). In our current study, we elected to use a mixture

of bile salts, reasoning that this strategy would more closely approximate what *V. cholerae* encounters *in vivo*. Our data suggest that bile salts disrupt the formation of the VqmA C134-C134 intermolecular disulfide bond. We do not know the mechanism by which this occurs. However, previous studies show that bile salts, specifically cholic acid (CHO) and deoxycholic acid (DOC), interfere with redox homeostasis in *Escherichia coli* by shifting the cellular environment to an oxidizing one and fostering disulfide bond formation in cytosolic proteins (43). In the context of our work, since VqmA intermolecular disulfide bond formation is disrupted, we propose that application of a bile salts mixture to *V. cholerae* causes reductive stress. Consistent with this idea, taurocholate binds to and inhibits DsbA, a protein required for the introduction of disulfide bonds in periplasmic proteins (24). We currently do not know whether incubation of *V. cholerae* with CHO and DOC, rather than a bile salts mixture, would drive phenotypes mimicking those observed in *E. coli*.

What advantage does *V. cholerae* accrue by using the regulatory program uncovered in our study? We propose that *V. cholerae* uses the different blends of AIs it encounters along with environmental modulation of VqmA activity to gauge its changing locations in the host. Thus, VqmA functions rather like a GPS device. In response to the information obtained about its microenvironment through VqmA, *V. cholerae* can appropriately tune its gene expression in space and time. We say this because, prior to entry into the small intestine (the site of cholera disease), *V. cholerae* will encounter oxygen limitation in the stomach. However, premature expression of virulence genes in the stomach, in the face of low pH and antimicrobial peptides, would be unproductive and, moreover, divert energy from combating host defense systems. Thus, increased VqmA activity, due to enhanced accumulation of DPO under anoxia coupled with formation of the C134-C134 intermolecular disulfide bond and suppression of formation of the activity-dampening intramolecular disulfide bond, will increase production of VqmR and, in turn, repress expression of genes involved in biofilm formation and virulence. Anoxia and the concurrent presence of bile, encountered upon entry into the host duodenum (upper region of the small intestine), may provide a spatially relevant signal to alert *V. cholerae* to begin to express virulence genes. In this case, bile salt-mediated inhibition of VqmA activity due to prevention of formation of the intermolecular disulfide bond will decrease VqmR production and, in turn, enhance expression of genes involved in biofilm formation and virulence. The combined use of bile salts and anoxia to decrease and increase VqmA activity, respectively, is also noteworthy because, as *V. cholerae* proceeds further through the intestinal tract, concentrations of bile salts decrease near the ileum (lower portion of the small intestine), where ~95% of bile salts are reabsorbed, and they reach a minimum in the large intestine. In contrast, anoxia is maintained throughout the intestinal tract. During successful infection, *V. cholerae* cell numbers increase as disease progresses. Accumulation of DPO should track with increasing cell density. Thus, it is possible that late in infection, *V. cholerae* resides in a high-DPO, anoxic environment lacking bile salts, conditions enabling reengagement of the VqmA-VqmR-DPO circuit, termination of virulence factor production, and expulsion from the host. In this context, we also note that DPO production by *V. cholerae* requires threonine as a substrate. Mucin is a major constituent of the intestinal tract and is composed of ~35% threonine (62). Intriguingly, both the stomach and large intestine, locations where *V. cholerae* typically does not reside, contain more mucus-secreting glands and mucus layers than does the small intestine (62). Thus, it is likely that enhanced access to mucus-derived threonine in the large intestine allows *V. cholerae* to increase DPO production. Again, high DPO levels repress virulence and biofilm formation. Thus, increased DPO production in the large intestine would foster *V. cholerae* departure from the host. We speculate that, in addition to oxygen and bile salts, the presence of mucus or threonine or the ability to synthesize DPO is also leveraged by *V. cholerae* as an additional spatial cue to optimize host dispersal timing.

MATERIALS AND METHODS

Materials. iProof DNA polymerase was purchased from Bio-Rad. Gel purification, plasmid preparation, RNA preparation (RNeasy), RNA-Protect reagents, qRT-PCR kits, and deoxynucleoside triphosphates were purchased from Qiagen. Antibodies were purchased from Sigma. Chitin flakes were supplied by Alfa Aesar. Instant Ocean (IO) sea salts came from Tetra Fish. Bile salts were purchased from Fluka.

Bacterial growth. *Escherichia coli* Top10 was used for cloning, *E. coli* S17-1 λ pir was used for conjugations, and *E. coli* BL21(DE3) was used for protein purification. *V. cholerae* and *E. coli* strains were grown in LB medium or in M9 minimal medium with glucose at 37°C, with shaking. When required, media were supplemented with streptomycin, 500 μ g/ml; kanamycin, 50 μ g/ml; spectinomycin, 200 μ g/ml; polymyxin B, 50 μ g/ml; and chloramphenicol, 1 μ g/ml. For bioluminescence assays, *V. cholerae* strains were cultured in SOC medium supplemented with tetracycline, and for AI-2 measurements, with boric acid (20 μ M). Unless otherwise indicated, bile salts were supplemented at 0.5% (vol/vol) and DPO at 25 μ M. Where indicated, oxygen deprivation was achieved as follows: (a) medium was sparged prior to use for at least 20 min with nitrogen gas, and (b) medium was incubated overnight with constant stirring inside a Coy anaerobic chamber equipped with a catalyst to scavenge oxygen. For both strategies a and b, subsequent steps were conducted inside the Coy anaerobic chamber, and (c) exponentially growing cells were transferred into capped microcentrifuge tubes with a headspace-to-volume ratio (HV ratio) of zero, and anaerobiosis was verified by the addition of 0.001% resazurin to control tubes, as described previously (63, 64). Microaerobiosis was achieved at ~10 min postshift and anaerobiosis by ~15 to 18 min postshift under these conditions, consistent with previous observations (63). Experiments presented in Fig. 1 were conducted using strategies a and b. Experiments described below used strategy c. In control experiments, we verified that our data were not altered due to differences in growth in the presence or absence of oxygen (see Fig. S1B in the supplemental material). Experiments in Fig. 1 were performed following *V. cholerae* growth in LB medium, which supports production of CAI-1, AI-2, and DPO. When grown in M9 minimal medium (Fig. 3 and 6), *V. cholerae* does not produce DPO because supplementation with threonine is required (11). Finally, we note that *V. cholerae* produces ~1 to 2 μ M DPO. In *in vivo* experiments, we treated cells with DPO at levels from 0 to 100 μ M, and in *in vitro* experiments we used the fixed concentration of 25 μ M. The goal was to assay DPO responses from far below to well above the 50% effective concentration (EC_{50}) *in vivo*, and in the *in vitro* experiments, to ensure that VqmA was always saturated with ligand.

Strain construction. (i) Chromosomal alterations. *V. cholerae* strains (Tables S1 and S2) were constructed using natural-transformation-mediated multiplexed-genome editing (MuGENT) (65, 66). Unless otherwise stated, chromosomal DNA from *V. cholerae* C6706 5m' was used as a template for PCRs. DNA fragments containing ~3 kb of homology to the upstream and downstream regions of the desired chromosomal region were generated using PCR. When necessary, splicing by overhang extension (SOE) PCR was used to combine multiple fragments of DNA, in which each fragment typically contained ~27 to 30 bp of overhang homology (65, 66). Antibiotic resistance cassettes, to facilitate selection of transformants following the MuGENT step, were designed to integrate at a neutral locus (*vc1807*) and were gifts from the Dalia group (Indiana University) (65, 66). *V. cholerae* cultures for use in natural transformations were prepared by inoculating 1 ml liquid LB medium from freezer stocks and growing the cells to an OD_{600} of ~1. Cells were pelleted at maximum speed in a microcentrifuge and resuspended at the original volume in 1 \times IO sea salts (7 g/liter). Competence was induced by combining a 75 μ l aliquot of the cell suspension with 900 μ l of a chitin IO mixture (8 g/liter chitin), and the preparation was incubated overnight at 30°C. The next day, these mixtures were supplemented with one (or multiple) PCR-amplified linear DNA fragment(s) of interest, as well as DNA encoding an antibiotic resistance cassette (65, 66). These mixtures were incubated overnight at 30°C, followed by vortex for 10 min. Next, 150 μ l of the suspension was plated onto solid LB medium containing the appropriate antibiotics followed by overnight incubation at 30°C. Resulting transformants were passaged three times on solid LB medium with antibiotics for purification. Genomic DNA from recombinant strains was used as a template for PCR to generate DNA fragments for future cotransformation, when necessary.

Site-directed mutations in *vqmA* were constructed by incorporating the desired alteration into forward or reverse PCR primers and generating DNA fragments with homology to DNA flanking chromosomal *vqmA*. These fragments were transformed, as described above, into a strain carrying *vqmA::kan* and the *vqmR-lacZ* transcriptional reporter integrated onto the chromosome. Clones were selected by screening for loss of kanamycin resistance and/or by assessment of positive LacZ activity when plated on agar containing 50 μ g/ml 5-bromo-4-chloro-3-indolyl- β -D-galactopyranoside (X-Gal).

(ii) Plasmid construction. DNA cloned into the pBAD-pEVS or pEVS plasmids (Tables S1 and S2) was assembled using enzyme-free XthA-dependent *in vivo* recombination cloning, as previously described (67, 68). Briefly, linear insert DNA fragments containing 30 bp of overlapping homology were generated using PCR. The plasmid backbone was likewise linearized by PCR amplification. All DNA fragments were gel purified and eluted in double-distilled water (ddH₂O). Thereafter, 80 ng of the backbone and 240 ng of each insert DNA fragment were combined and incubated for 1 h at room temperature followed by transformation and clone recovery in chemically competent Top10 *E. coli* cells. Constructs in the pET15b backbone were assembled using traditional restriction-enzyme cloning using primers and protocols described earlier (15).

Assessing protein abundance and formation of disulfide bonds. Strains cultured overnight in LB medium (~16 to 18 h) were diluted into fresh M9 minimal medium, with antibiotics, as necessary, to a final OD_{600} of 0.004. When assessing levels of VqmA-FLAG produced from the chromosomally integrated *vqmA-FLAG* construct, strains were cultured to an OD_{600} of ~0.3 (~4 h of growth) and cells were harvested by centrifugation. For strains requiring induction of protein expression, 0.2% arabinose was

added to the culture medium at 4 h postinoculation, and growth was continued for an additional 1 h, at which point the cultures were divided and portions were supplemented with 25 μ M DPO and/or 0.5% bile salts and/or deprived of oxygen. Treatments were continued for another 1 h, after which cells were harvested by centrifugation at 13,000 rpm and the pellets were immediately frozen at -80°C until use.

Immunoblotting. Cells were resuspended in ice-cold phosphate-buffered saline (PBS) and diluted to a final OD_{600} of 7 for protein produced from the chromosome or to an OD_{600} of 3.5 for protein produced from a plasmid, in a volume of 20 μ l. The cells were lysed by addition of 5 μ l Bugbuster (Novagen) supplemented with 1 μ g lysozyme and 25 U/ml benzonase. Samples were combined with SDS-PAGE buffer in the presence or absence of BME (100 mM) and boiled for 20 min, and proteins were separated on 4 to 20% Mini-Protein TGX gels (Bio-Rad). Proteins were transferred to polyvinylidene difluoride (PVDF) membranes (Bio-Rad) for 1 h at 4°C at 100 V. Membranes were blocked overnight in PBST (1 \times PBS, 0.03% Tween 20) supplemented with 5% milk, washed 5 times with PBST, and incubated for 40 min with 1:5,000 dilution of monoclonal anti-FLAG-peroxidase antibody (Sigma) in PBST. The membranes were subsequently washed another five times with PBST. FLAG epitope-tagged protein levels were visualized using the Amersham ECL Western blotting detection reagent (GE Healthcare). Thereafter, the antibody was removed by 2 serial incubations in stripping buffer (15 g/liter glycine, 1 g/liter SDS, 10 ml/liter Tween 20, pH 2.2) for 5 min each. The membrane was reequilibrated by 4 washes in PBST, 20 min each, and used to detect the abundance of the loading control, RNA polymerase α . Washes and incubations as described above were performed to enable antibody binding and removal of excess. The primary antibody, anti-*E. coli* RNA polymerase α (Biolegend), and the secondary antibody, anti-mouse IgG horseradish peroxidase (HRP) conjugate antibody (Promega), were both used at a 1:10,000 dilution. In all cases, protein levels were quantified using Image J software.

Protein purification. pET15b plasmids encoding 6 \times His-VqmA were mobilized into Δ *tdh E. coli* BL21(DE3). Strains were cultured for protein production as described previously (15, 16). Cells were harvested by centrifugation, and pellets were resuspended in 1/100 volume of lysis buffer (50 mM Tris, 150 mM NaCl, pH 7.5, containing 0.5 mg/ml lysozyme, 1 \times protease inhibitor, and benzonase) for 5 min followed by the addition of an equal volume of Bugbuster reagent (Novagen). The cell lysate was clarified by centrifugation at 13,000 rpm, and protein was purified using Ni-NTA superflow resin (Qiagen), according to the manufacturer's recommendations for a centrifugation-based protocol, except that the loading and wash buffers all contained 1 to 5 mM imidazole to decrease nonspecific protein binding. The protein was eluted from the resin using 300 mM imidazole and thereafter dialyzed twice against 50 mM Tris, 150 mM NaCl, pH 7.5, using a Slide-A-Lyzer module (Thermo Fisher). When necessary, buffers were amended with 5 mM DTT. To purify Holo-VqmA, buffers were supplemented with 100 μ M DPO.

EMSAs. The DNA corresponding to the promoter region of *vqmR*, \sim 100 bp, was amplified using *V. cholerae* genomic DNA as a template. Where mentioned, protein was pretreated in binding buffer with 10-fold molar excess DTT or diamide in order to reduce or oxidize the protein, respectively. To initiate electromobility gel shift assays (EMSAs), 0.2 to 3.5 μ M protein was combined with 30 ng probe DNA in binding buffer (50 mM Tris-HCl, pH 8, 150 mM NaCl). Reactions were allowed to proceed at room temperature (RT) for 15 min. Samples were separated on a Novex 6% DNA retardation gel (Thermo) by electrophoresis in 1 \times Tris-buffered EDTA (TBE) at 100 V. Gels were subsequently incubated with Sybr green reagent, diluted in 1 \times TBE at RT for 25 min, washed with five successive rounds of ddH_2O , and imaged using an ImageQuant LAS 4000 imager and the Sybr green channel setting.

Analysis of relative AI levels in conditioned growth medium following aerobic or anaerobic growth. *V. cholerae* strains were cultured overnight in LB medium (\sim 16 to 18 h) and diluted into fresh aerobic or anaerobic LB medium to a final OD_{600} of 0.004. The cultures were incubated at 37°C for an additional \sim 6 h with shaking. The cells were removed by centrifugation at 13,000 rpm, and the spent medium was filtered through 0.2- μ m filters. Twenty percent (vol/vol) 5 \times LB was added to the spent medium preparations (here designated reconditioned spent medium). Negative controls consisted of spent medium prepared from strains incapable of synthesizing CAI-1, AI-2, and DPO. Subsequently, reconditioned spent medium was combined with *V. cholerae* reporter strains expressing only a single QS receptor that, therefore, detect only one AI. In the case of CAI-1 and AI-2 detection, the reporter strains carried a plasmid encoding the *Vibrio harveyi luxCDABE* (luciferase) operon (2). For DPO detection, the reporter strain possessed a *pvqmR-lux* (luciferase) fusion on the chromosome in place of the native *lacZ* locus (16). Genotypes are provided in Table S1 in the supplemental material. The reporter strains and reconditioned spent medium preparations were combined to a final volume of 150 μ l in wells of 96-well plates, covered with Breathe-Easy film, and incubated at 30°C with shaking for 2.5 to 4 h. Finally, bioluminescence and OD_{600} values were recorded. Relative light units (RLUs) were defined as light production (counts per minute) divided by OD_{600} . Normalized RLUs were obtained by subtraction of the RLU values obtained from the negative controls.

Beta-galactosidase assays. *V. cholerae* strains cultured overnight in LB medium were diluted into fresh M9 medium to a final OD_{600} of 0.004 and thereafter cultured to an OD_{600} of \sim 0.3 (\sim 4 h). The cultures were held on ice prior to assay or subjected to further treatments, as described below. For strains requiring inducible protein expression, 0.01% arabinose was added to the culture medium at 4 h postinoculation and growth was continued for an additional 1 h. In all cases, cultures were divided into aliquots and individual portions were supplemented with 25 μ M DPO and/or 0.5% bile salts and/or deprived of oxygen. Cells were cultured for an additional 1 h and then held on ice prior to assay. To assess the effect of reductant, at 2 h postinoculation, the cultures were supplemented with 300 μ M DTT. Cells were cultured for another 2 h to allow DTT permeation, before *vqmA* expression was induced by the addition of arabinose. Subsequent treatments were as described above. LacZ activity assays were carried out as follows: cells were combined 1:1 (vol/vol) with Bugbuster reagent for 20 min. The assay was

initiated by combining 20 μ l of the cell-Bugbuster mixture with 140 μ l of assay buffer (80% Bugbuster, 10% 10 \times PBS, 1 mM MgSO₄, 10 μ g/ml lysozyme, benzonase [0.05%, vol/vol], β -mercaptoethanol [0.1%, vol/vol], 67 μ g/ml fluorescein-di- β -D-galactopyranoside). Changes in fluorescence were captured using the GFP channel on a Synergy Neo2 HTS multimode microplate reader. Activity units were defined as the change in fluorescence/minute/OD₆₀₀ of the culture at the point of harvest.

RNA isolation and quantitative RT-PCR. Strains cultured overnight in LB were diluted into fresh M9 minimal medium to a final OD₆₀₀ of 0.004. Next, the strains were grown to an OD₆₀₀ of \sim 0.3 (\sim 4 h postinoculation) with shaking at 37°C, at which point the cultures were divided into portions that were supplemented with 25 μ M DPO and/or 0.5% bile salts and/or deprived of oxygen. Treatments were continued for another 1 h, and the cells were harvested and treated for 15 min at room temperature with RNAProtect reagent, per the manufacturer's instructions. RNA was isolated using the RNeasy kit (Qiagen), and 2 μ g of total RNA was depleted of contaminating DNA using Turbo DNase (Applied Biosystems), using the manufacturer's recommended protocol. Five hundred nanograms of the resulting total RNA was used to construct cDNA libraries using SuperScript III reverse transcriptase (Invitrogen). qPCR was conducted using the PerfeCTa SYBR green FastMix Low ROX (Quanta Biosciences) reagent.

Caco-2 culture and coculture with bile salts and V. cholerae. The HTB37 cell line was obtained from ATCC and thereafter cultured and passaged in Eagle's minimum essential medium (EMEM) (ATCC) supplemented with 10% fetal bovine serum (FBS) (Thermo Fisher), 2 mM glutamine (Thermo Fisher), 1 \times penicillin-streptomycin (Pen-Strep) (Thermo Fisher), and 2.5 μ g/ml plasmocin (Invitrogen), per ATCC recommendations. Prior to coculture, Caco-2 cells were seeded at 0.32 cm² into a tissue culture-treated 96-well plate in EMEM, as described above, except that the 2 mM glutamine was not included. The cells were cultured to confluence, the medium was removed by aspiration, and the cells were washed with Earle's balanced salt solution followed by the addition of EMEM containing 25 μ M DPO but lacking antibiotics/glutamine/FBS. At time zero, *V. cholerae*, grown as described below, was added, at a multiplicity of infection (MOI) of 10 and with 0.05% bile salts. Following coculture for 3.5 h, the medium and the bacteria were removed by aspiration, the wells were washed with Earle's balanced salt solution, and Caco-2 cell viability was assessed using the neutral red assay (69). For coculture with Caco-2 cells, *V. cholerae* WT and Δ vqmA strains were cultured overnight under static conditions in AKI medium containing 25 μ M DPO in tubes with an HV ratio of zero at 37°C. The next day, the cells were decanted into glass tubes and cultured with vigorous shaking for 1 h. Subsequently, the cultures were diluted with PBS to the appropriate density and added to the Caco-2 cells.

SUPPLEMENTAL MATERIAL

Supplemental material is available online only.

TEXT S1, DOCX file, 0.03 MB.

FIG S1, TIF file, 1 MB.

FIG S2, TIF file, 1.6 MB.

FIG S3, TIF file, 2.8 MB.

FIG S4, TIF file, 1 MB.

FIG S5, TIF file, 1.3 MB.

FIG S6, TIF file, 1.8 MB.

FIG S7, TIF file, 1.2 MB.

TABLE S1, DOCX file, 0.03 MB.

TABLE S2, DOCX file, 0.03 MB.

ACKNOWLEDGMENTS

We thank the Donia lab for generously allowing us to use their anaerobic chamber. We thank Ankur Dalia for the gift of protocols, strains, and reagents to facilitate MuGENT cloning. We thank Tharan Srikumar, Saw Kyin, and Henry Shwe for help with mass spectroscopy experiments.

This work was supported by the Howard Hughes Medical Institute, National Science Foundation grant MCB-1713731, and NIH grant 5R37GM065859 to B.L.B. A.A.M. is a Howard Hughes Medical Institute Fellow of the Life Sciences Research Institute.

The authors have no competing interests to declare.

REFERENCES

1. Hammer BK, Bassler BL. 2003. Quorum sensing controls biofilm formation in *Vibrio cholerae*. *Mol Microbiol* 50:101–104. <https://doi.org/10.1046/j.1365-2958.2003.03688.x>
2. Miller MB, Skorupski K, Lenz DH, Taylor RK, Bassler BL. 2002. Parallel quorum sensing systems converge to regulate virulence in *Vibrio cholerae*. *Cell* 110:303–314. [https://doi.org/10.1016/S0092-8674\(02\)00829-2](https://doi.org/10.1016/S0092-8674(02)00829-2).
3. Papenfort K, Bassler BL. 2016. Quorum sensing signal-response systems in Gram-negative bacteria. *Nat Rev Microbiol* 14:576–588. <https://doi.org/10.1038/nrmicro.2016.89>.
4. Suckow G, Seitz P, Blokesch M. 2011. Quorum sensing contributes to natural transformation of *Vibrio cholerae* in a species-specific manner. *J Bacteriol* 193:4914–4924. <https://doi.org/10.1128/JB.05396-11>.
5. Schauder S, Bassler BL. 2001. The languages of bacteria. *Genes Dev* 15:1468–1480. <https://doi.org/10.1101/gad.899601>.

6. Waters CM, Bassler BL. 2005. Quorum sensing: cell-to-cell communication in bacteria. *Annu Rev Cell Dev Biol* 21:319–346. <https://doi.org/10.1146/annurev.cellbio.21.012704.131001>.
7. Jung SA, Chapman CA, Ng WL. 2015. Quadruple quorum-sensing inputs control *Vibrio cholerae* virulence and maintain system robustness. *PLoS Pathog* 11:e1004837. <https://doi.org/10.1371/journal.ppat.1004837>.
8. Zhu J, Mekalanos JJ. 2003. Quorum sensing-dependent biofilms enhance colonization in *Vibrio cholerae*. *Dev Cell* 5:647–656. [https://doi.org/10.1016/S1534-5807\(03\)00295-8](https://doi.org/10.1016/S1534-5807(03)00295-8).
9. Zhu J, Miller MB, Vance RE, Dziejman M, Bassler BL, Mekalanos JJ. 2002. Quorum-sensing regulators control virulence gene expression in *Vibrio cholerae*. *Proc Natl Acad Sci U S A* 99:3129–3134. <https://doi.org/10.1073/pnas.052694299>.
10. Higgins DA, Pomianek ME, Kraml CM, Taylor RK, Semmelhack MF, Bassler BL. 2007. The major *Vibrio cholerae* autoinducer and its role in virulence factor production. *Nature* 450:883–886. <https://doi.org/10.1038/nature06284>.
11. Papenfort K, Silpe JE, Schramma KR, Cong JP, Seyedsayamdost MR, Bassler BL. 2017. A *Vibrio cholerae* autoinducer-receptor pair that controls biofilm formation. *Nat Chem Biol* 13:551–557. <https://doi.org/10.1038/nchembio.2336>.
12. Schauder S, Shokat K, Surette MG, Bassler BL. 2001. The LuxS family of bacterial autoinducers: biosynthesis of a novel quorum-sensing signal molecule. *Mol Microbiol* 41:463–476. <https://doi.org/10.1046/j.1365-2958.2001.02532.x>.
13. Bridges AA, Bassler BL. 2019. The intragenus and interspecies quorum-sensing autoinducers exert distinct control over *Vibrio cholerae* biofilm formation and dispersal. *PLoS Biol* 17:e3000429. <https://doi.org/10.1371/journal.pbio.3000429>.
14. Liu Z, Hsiao A, Joëlsson A, Zhu J. 2006. The transcriptional regulator VqmA increases expression of the quorum-sensing activator HapR in *Vibrio cholerae*. *J Bacteriol* 188:2446–2453. <https://doi.org/10.1128/JB.188.7.2446-2453.2006>.
15. Papenfort K, Forstner KU, Cong JP, Sharma CM, Bassler BL. 2015. Differential RNA-seq of *Vibrio cholerae* identifies the VqmR small RNA as a regulator of biofilm formation. *Proc Natl Acad Sci U S A* 112:E766–E775. <https://doi.org/10.1073/pnas.1500203112>.
16. Huang X, Duddy OP, Silpe JE, Paczkowski JE, Cong J, Henke BR, Bassler BL. 2020. Mechanism underlying autoinducer recognition in the *Vibrio cholerae* DPO-VqmA quorum-sensing pathway. *J Biol Chem* 295:2916–2931. <https://doi.org/10.1074/jbc.RA119.012104>.
17. Escobar LE, Ryan SJ, Stewart-Ibarra AM, Finkelstein JL, King CA, Qiao H, Polhemus ME. 2015. A global map of suitability for coastal *Vibrio cholerae* under current and future climate conditions. *Acta Trop* 149:202–211. <https://doi.org/10.1016/j.actatropica.2015.05.028>.
18. Zheng L, Kelly CJ, Colgan SP. 2015. Physiologic hypoxia and oxygen homeostasis in the healthy intestine. A review in the theme: cellular responses to hypoxia. *Am J Physiol Cell Physiol* 309:C350–C360. <https://doi.org/10.1152/ajpcell.00191.2015>.
19. Dawson PA. 1998. Bile secretion and the enterohepatic circulation of bile acids, p 1052–1063. *In* Feldman M, Sleisenger MH, Scharschmidt BF (ed), Sleisenger and Fordtran's gastrointestinal and liver disease: pathophysiology/diagnosis/management, 6th ed. WB Saunders Co, Philadelphia, PA.
20. Chatterjee A, Dutta PK, Chowdhury R. 2007. Effect of fatty acids and cholesterol present in bile on expression of virulence factors and motility of *Vibrio cholerae*. *Infect Immun* 75:1946–1953. <https://doi.org/10.1128/IAI.01435-06>.
21. Childers BM, Cao X, Weber GG, Demeler B, Hart PJ, Klose KE. 2011. N-terminal residues of the *Vibrio cholerae* virulence regulatory protein ToxT involved in dimerization and modulation by fatty acids. *J Biol Chem* 286:28644–28655. <https://doi.org/10.1074/jbc.M111.258780>.
22. Hung DT, Mekalanos JJ. 2005. Bile acids induce cholera toxin expression in *Vibrio cholerae* in a ToxT-independent manner. *Proc Natl Acad Sci U S A* 102:3028–3033. <https://doi.org/10.1073/pnas.040959102>.
23. Weber GG, Klose KE. 2011. The complexity of ToxT-dependent transcription in *Vibrio cholerae*. *Indian J Med Res* 133:201–206.
24. Xue Y, Tu F, Shi M, Wu CQ, Ren G, Wang X, Fang W, Song H, Yang M. 2016. Redox pathway sensing bile salts activates virulence gene expression in *Vibrio cholerae*. *Mol Microbiol* 102:909–924. <https://doi.org/10.1111/mmi.13497>.
25. Yang M, Liu Z, Hughes C, Stern AM, Wang H, Zhong Z, Kan B, Fenical W, Zhu J. 2013. Bile salt-induced intermolecular disulfide bond formation activates *Vibrio cholerae* virulence. *Proc Natl Acad Sci U S A* 110:2348–2353. <https://doi.org/10.1073/pnas.1218039110>.
26. Hung DT, Zhu J, Sturtevant D, Mekalanos JJ. 2006. Bile acids stimulate biofilm formation in *Vibrio cholerae*. *Mol Microbiol* 59:193–201. <https://doi.org/10.1111/j.1365-2958.2005.04846.x>.
27. Koestler BJ, Waters CM. 2014. Bile acids and bicarbonate inversely regulate intracellular cyclic di-GMP in *Vibrio cholerae*. *Infect Immun* 82:3002–3014. <https://doi.org/10.1128/IAI.01664-14>.
28. Wu H, Li M, Peng C, Yin Y, Guo H, Wang W, Xu Q, Zhou H, Xu C, Yu F, He J. 2019. Large conformation shifts of *Vibrio cholerae* VqmA dimer in the absence of target DNA provide insight into DNA-binding mechanisms of LuxR-type receptors. *Biochem Biophys Res Commun* 520:399–405. <https://doi.org/10.1016/j.bbrc.2019.10.063>.
29. Braun M, Thony-Meyer L. 2005. Cytochrome c maturation and the physiological role of c-type cytochromes in *Vibrio cholerae*. *J Bacteriol* 187:5996–6004. <https://doi.org/10.1128/JB.187.17.5996-6004.2005>.
30. Liu Z, Yang M, Peterfreund GL, Tsou AM, Selamoglu N, Daldal F, Zhong Z, Kan B, Zhu J. 2011. *Vibrio cholerae* anaerobic induction of virulence gene expression is controlled by thiol-based switches of virulence regulator AphB. *Proc Natl Acad Sci U S A* 108:810–815. <https://doi.org/10.1073/pnas.1014640108>.
31. Muras V, Dogaru-Kinn P, Minato Y, Häse CC, Steuber J. 2016. The Na⁺-translocating NADH:Quinone oxidoreductase enhances oxidative stress in the cytoplasm of *Vibrio cholerae*. *J Bacteriol* 198:2307–2317. <https://doi.org/10.1128/JB.00342-16>.
32. Oktyabrskii ON, Smirnova GV. 2012. Redox potential changes in bacterial cultures under stress conditions. *Microbiology* 81:131–142. <https://doi.org/10.1134/S0026261712020099>.
33. Masuda S, Dong C, Swem D, Setterdahl AT, Knaff DB, Bauer CE. 2002. Repression of photosynthesis gene expression by formation of a disulfide bond in CrtJ. *Proc Natl Acad Sci U S A* 99:7078–7083. <https://doi.org/10.1073/pnas.102013099>.
34. Antelmann H, Helmann JD. 2011. Thiol-based redox switches and gene regulation. *Antioxid Redox Signal* 14:1049–1063. <https://doi.org/10.1089/ars.2010.3400>.
35. Parashar V, Aggarwal C, Federle MJ, Neiditch MB. 2015. Rgg protein structure-function and inhibition by cyclic peptide compounds. *Proc Natl Acad Sci U S A* 112:5177–5182. <https://doi.org/10.1073/pnas.1500357112>.
36. Bardwell JC, McGovern K, Beckwith J. 1991. Identification of a protein required for disulfide bond formation *in vivo*. *Cell* 67:581–589. [https://doi.org/10.1016/0092-8674\(91\)90532-4](https://doi.org/10.1016/0092-8674(91)90532-4).
37. Scheele G, Jacoby R. 1982. Conformational changes associated with proteolytic processing of presecretory proteins allow glutathione-catalyzed formation of native disulfide bonds. *J Biol Chem* 257:12277–12282.
38. Falke JJ, Koshland DE, Jr. 1987. Global flexibility in a sensory receptor: a site-directed cross-linking approach. *Science* 237:1596–1600. <https://doi.org/10.1126/science.2820061>.
39. Ottemann KM, Mekalanos JJ. 1996. The ToxR protein of *Vibrio cholerae* forms homodimers and heterodimers. *J Bacteriol* 178:156–162. <https://doi.org/10.1128/jb.178.1.156-162.1996>.
40. Landeta C, McPartland L, Tran NQ, Meehan BM, Zhang Y, Tanweer Z, Wakabayashi S, Rock J, Kim T, Balasubramanian D, Audette R, Toosky M, Pinkham J, Rubin EJ, Lory S, Pier G, Boyd D, Beckwith J. 2019. Inhibition of *Pseudomonas aeruginosa* and *Mycobacterium tuberculosis* disulfide bond forming enzymes. *Mol Microbiol* 111:918–937. <https://doi.org/10.1111/mmi.14185>.
41. Rossius M, Hochgrafe F, Antelmann H. 2018. Thiol-redox proteomics to study reversible protein thiol oxidations in bacteria. *Methods Mol Biol* 1841:261–275. https://doi.org/10.1007/978-1-4939-8695-8_18.
42. Kosower NS, Kosower EM. 1995. Diamide: an oxidant probe for thiols. *Methods Enzymol* 251:123–133. [https://doi.org/10.1016/0076-6879\(95\)51116-4](https://doi.org/10.1016/0076-6879(95)51116-4).
43. Creemers CM, Knoefler D, Vitvitsky V, Banerjee R, Jakob U. 2014. Bile salts act as effective protein-unfolding agents and instigators of disulfide stress *in vivo*. *Proc Natl Acad Sci U S A* 111:E1610–E1619. <https://doi.org/10.1073/pnas.1401941111>.
44. Fong JCN, Syed KA, Klose KE, Yildiz FH. 2010. Role of *Vibrio* polysaccharide (*vps*) genes in VPS production, biofilm formation and *Vibrio cholerae* pathogenesis. *Microbiology* 156:2757–2769. <https://doi.org/10.1099/mic.0.040196-0>.
45. Taylor RK, Miller VL, Furlong DB, Mekalanos JJ. 1987. Use of *phoA* gene fusions to identify a pilus colonization factor coordinately regulated with cholera toxin. *Proc Natl Acad Sci U S A* 84:2833–2837. <https://doi.org/10.1073/pnas.84.9.2833>.
46. Joëlsson A, Kan B, Zhu J. 2007. Quorum sensing enhances the stress

- response in *Vibrio cholerae*. *Appl Environ Microbiol* 73:3742–3746. <https://doi.org/10.1128/AEM.02804-06>.
47. Pereira CS, Thompson JA, Xavier KB. 2013. AI-2-mediated signalling in bacteria. *FEMS Microbiol Rev* 37:156–181. <https://doi.org/10.1111/j.1574-6976.2012.00345.x>.
 48. Chen X, Schauder S, Potier N, Van Dorselaer A, Pelczar I, Bassler BL, Hughson FM. 2002. Structural identification of a bacterial quorum-sensing signal containing boron. *Nature* 415:545–549. <https://doi.org/10.1038/415545a>.
 49. Kelly RC, Bolitho ME, Higgins DA, Lu W, Ng WL, Jeffrey PD, Rabinowitz JD, Semmelhack MF, Hughson FM, Bassler BL. 2009. The *Vibrio cholerae* quorum-sensing autoinducer CAI-1: analysis of the biosynthetic enzyme CqsA. *Nat Chem Biol* 5:891–895. <https://doi.org/10.1038/nchembio.237>.
 50. Winzer K, Hardie KR, Burgess N, Doherty N, Kirke D, Holden MTG, Linforth R, Cornell KA, Taylor AJ, Hill PJ, Williams P. 2002. LuxS: its role in central metabolism and the *in vitro* synthesis of 4-hydroxy-5-methyl-3(2H)-furanone. *Microbiology* 148:909–922. <https://doi.org/10.1099/00221287-148-4-909>.
 51. Krishnan HH, Ghosh A, Paul K, Chowdhury R. 2004. Effect of anaerobiosis on expression of virulence factors in *Vibrio cholerae*. *Infect Immun* 72:3961–3967. <https://doi.org/10.1128/IAI.72.7.3961-3967.2004>.
 52. Lee KM, Park Y, Bari W, Yoon MY, Go J, Kim SC, Lee HI, Yoon SS. 2012. Activation of cholera toxin production by anaerobic respiration of trimethylamine N-oxide in *Vibrio cholerae*. *J Biol Chem* 287:39742–39752. <https://doi.org/10.1074/jbc.M112.394932>.
 53. Wu H, Li M, Guo H, Zhou H, Li B, Xu Q, Xu C, Yu F, He J. 2019. Crystal structure of the *Vibrio cholerae* VqmA-ligand-DNA complex provides insight into ligand-binding mechanisms relevant for drug design. *J Biol Chem* 294:2580–2592. <https://doi.org/10.1074/jbc.RA118.006082>.
 54. Trotter EW, Grant CM. 2002. Thioredoxins are required for protection against a reductive stress in the yeast *Saccharomyces cerevisiae*. *Mol Microbiol* 46:869–878. <https://doi.org/10.1046/j.1365-2958.2002.03216.x>.
 55. Chen PR, Nishida S, Poor CB, Cheng A, Bae T, Kuechenmeister L, Dunman PM, Missiakas D, He C. 2009. A new oxidative sensing and regulation pathway mediated by the MgrA homologue SarZ in *Staphylococcus aureus*. *Mol Microbiol* 71:198–211. <https://doi.org/10.1111/j.1365-2958.2008.06518.x>.
 56. Cremers CM, Jakob U. 2013. Oxidant sensing by reversible disulfide bond formation. *J Biol Chem* 288:26489–26496. <https://doi.org/10.1074/jbc.R113.462929>.
 57. Zheng M, Aslund F, Storz G. 1998. Activation of the OxyR transcription factor by reversible disulfide bond formation. *Science* 279:1718–1721. <https://doi.org/10.1126/science.279.5357.1718>.
 58. García-Quintanilla M, Prieto AI, Barnes L, Ramos-Morales F, Casadesús J. 2006. Bile-induced curing of the virulence plasmid in *Salmonella enterica* serovar Typhimurium. *J Bacteriol* 188:7963–7965. <https://doi.org/10.1128/JB.00995-06>.
 59. Olive AJ, Kenjale R, Espina M, Moore DS, Picking WL, Picking WD. 2007. Bile salts stimulate recruitment of IpaB to the *Shigella flexneri* surface, where it colocalizes with IpaD at the tip of the type III secretion needle. *Infect Immun* 75:2626–2629. <https://doi.org/10.1128/IAI.01599-06>.
 60. Lowden MJ, Skorupski K, Pellegrini M, Chiorazzo MG, Taylor RK, Kull FJ. 2010. Structure of *Vibrio cholerae* ToxT reveals a mechanism for fatty acid regulation of virulence genes. *Proc Natl Acad Sci U S A* 107:2860–2865. <https://doi.org/10.1073/pnas.0915021107>.
 61. Plecha SC, Withey JH. 2015. Mechanism for inhibition of *Vibrio cholerae* ToxT activity by the unsaturated fatty acid components of bile. *J Bacteriol* 197:1716–1725. <https://doi.org/10.1128/JB.02409-14>.
 62. Johansson ME, Sjoval H, Hansson GC. 2013. The gastrointestinal mucus system in health and disease. *Nat Rev Gastroenterol Hepatol* 10:352–361. <https://doi.org/10.1038/nrgastro.2013.35>.
 63. Fuchs S, Pane-Farre J, Kohler C, Hecker M, Engelmann S. 2007. Anaerobic gene expression in *Staphylococcus aureus*. *J Bacteriol* 189:4275–4289. <https://doi.org/10.1128/JB.00081-07>.
 64. Mashruwala AA, Bhatt S, Poudel S, Boyd ES, Boyd JM. 2016. The DUF59 containing protein SufT is involved in the maturation of iron-sulfur (FeS) proteins during conditions of high FeS cofactor demand in *Staphylococcus aureus*. *PLoS Genet* 12:e1006233. <https://doi.org/10.1371/journal.pgen.1006233>.
 65. Dalia AB. 2018. Natural cotransformation and multiplex genome editing by natural transformation (MuGENT) of *Vibrio cholerae*. *Methods Mol Biol* 1839:53–64. https://doi.org/10.1007/978-1-4939-8685-9_6.
 66. Dalia AB, McDonough E, Camilli A. 2014. Multiplex genome editing by natural transformation. *Proc Natl Acad Sci U S A* 111:8937–8942. <https://doi.org/10.1073/pnas.1406478111>.
 67. Beyer HM, Gonschorek P, Samodelov SL, Meier M, Weber W, Zurbriggen MD. 2015. AQUA cloning: a versatile and simple enzyme-free cloning approach. *PLoS One* 10:e0137652. <https://doi.org/10.1371/journal.pone.0137652>.
 68. Nozaki S, Niki H. 2018. Exonuclease III (XthA) enforces *in vivo* DNA cloning of *Escherichia coli* to create cohesive ends. *J Bacteriol* 201:e00660-18. <https://doi.org/10.1128/JB.00660-18>.
 69. Repetto G, del Peso A, Zurita JL. 2008. Neutral red uptake assay for the estimation of cell viability/cytotoxicity. *Nat Protoc* 3:1125–1131. <https://doi.org/10.1038/nprot.2008.75>.